

## NOISE SOURCE IDENTIFICATION WITH INCREASED SPATIAL RESOLUTION

Svend Gade, Jørgen Hald and Bernard Ginn

*Brüel & Kjær Sound & Vibration Measurements A/S, Skodsborgvej 307, DK-2850 Nærum, DENMARK*

*e-mail: [Svend.Gade@bksv.com](mailto:Svend.Gade@bksv.com)*

Delay-and-sum (DAS) Planar Beamforming has been a widely used Noise Source Identification Technique for the last decade. It is a quick one shot measurement technique being able to map sources that are larger than the array itself. The spatial resolution is proportional to distance between array and source, and inversely proportional to wavelength, thus the resolution is only good at medium to high frequencies. Improved algorithms using iterative de-convolution techniques offers up to ten times better resolution. The principle behind these techniques is described in this paper, as well as measurement examples from the automotive industry are presented.

---

### 1. Introduction

Beamforming is an array-based measurement technique for sound-source location from medium to long measurement distances. Basically, the source location is performed by estimating the amplitudes of plane (or spherical) waves incident towards the array from a chosen set of directions. The angular resolution is inversely proportional to the array diameter measured in units of wavelength, so the array should be much larger than wavelength to get a fine angular resolution. At low frequencies, this requirement usually cannot be met, so here the resolution will be poor. For typical, irregular array designs, the beamforming method does not allow the measurement distance to be much smaller than the array diameter. On the other hand, the measurement distance should be kept as small as possible to achieve the finest possible resolution on the source surface. This is of course not possible when measuring on large objects. The use of a discrete set of measurement points on a plane can be seen as a spatial sampling of the sound field. Nearfield Acoustical Holography, NAH as well as SONAH (Statistically Optimized NAH) require a grid spacing less than half a wavelength at the highest frequency of interest<sup>(3)</sup>. At higher frequencies the number of measurement points gets very high. When the grid spacing exceeds half a wavelength, spatial aliasing components or interpolation errors quickly get very disturbing. Irregular arrays on the other hand can potentially provide a much smoother transition: spatial aliasing effects can be kept at an acceptable level up to a much higher frequency with the same average spatial sampling density. This indicates why beamforming can measure up to high frequencies and provide a good resolution with a fairly low number of microphones. Thus beamforming is an attractive alternative and supplement to NAH/SONAH, because measurements can be taken at some intermediate distance with a highly sparse array, which is not required to be larger than the noise source. And at high frequencies beamforming can provide quite good resolution.

## 2. Theory of Beamforming

As illustrated in Fig. 1, we consider a planar array of  $M$  microphones at  $M$  distributed locations  $\mathbf{r}_m$  ( $m=1,2,\dots,M$ ) in the  $xy$ -plane of our coordinate system. When such an array is applied for Delay-and-Sum Beamforming, the measured pressure signals  $p_m$  are individually delayed and then summed <sup>(2)</sup>:

$$b(\boldsymbol{\kappa}, t) = \sum_{m=1}^M p_m(t - \Delta_m(\boldsymbol{\kappa})) \quad (1)$$

The individual time delays  $\Delta_m$  are chosen with the aim of achieving selective directional sensitivity in a specific direction, characterized here by a unit vector  $\boldsymbol{\kappa}$ . This objective is met by adjusting the time delays in such a way that signals associated with a plane wave, incident from the direction  $\boldsymbol{\kappa}$ , will be aligned in time before they are summed. Geometrical considerations (see Fig. 1) show that this can be obtained by choosing:

$$\Delta_m = \frac{\boldsymbol{\kappa} \cdot \mathbf{r}_m}{c} \quad (2)$$

where  $c$  is the propagation speed of sound. Signals arriving from other far-field directions will not be aligned before the summation, and therefore they will not coherently add up.

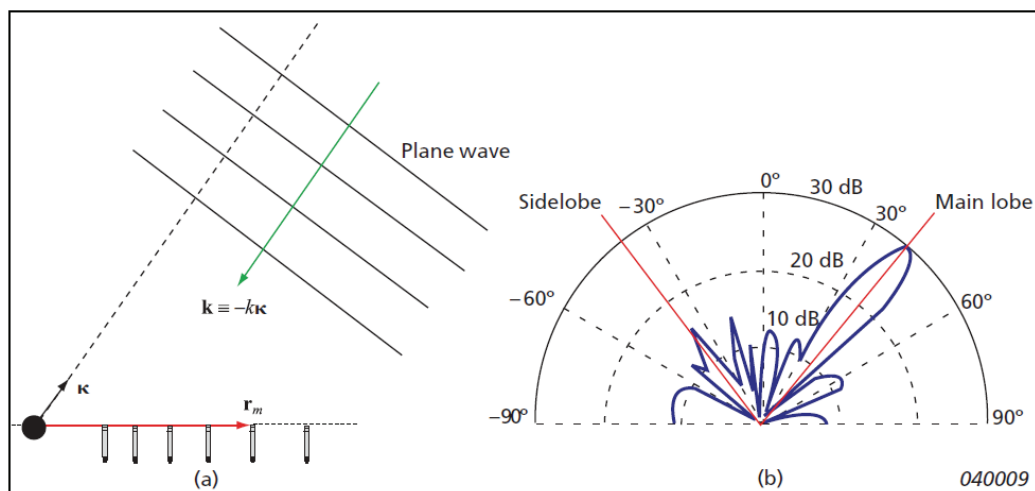


Fig. 1 – (a) A microphone array, a far-field focus direction, and a plane wave incident from the focus direction. (b) Directional sensitivity diagram with a main lobe in the focus direction and lower side lobes in other directions

The frequency domain version of Eq. (1) for the Delay-and-Sum beamformer output is:

$$B(\mathbf{\kappa}, \omega) = \sum_{m=1}^M P_m(\omega) \cdot e^{-j\omega\Delta_m(\mathbf{\kappa})} = \sum_{m=1}^M P_m(\omega) \cdot e^{j\mathbf{k}\cdot\mathbf{r}_m} \quad (3)$$

Here,  $\omega$  is the temporal angular frequency,  $\mathbf{k} \equiv -k\mathbf{\kappa}$  is the wave number vector of a plane wave incident from the direction  $\mathbf{\kappa}$  in which the array is focused – see Fig. 1 – and  $k=\omega/c$  is the wave number. In Eq. (3) an implicit time factor equal to  $e^{j\omega t}$  is assumed.

The width of the main lobe of the Array Pattern can be estimated from the similarity of the Eq. (3) with a 2D DFT of a “rectangular” type of spatial window function covering the area of the array: The main lobe width will be inversely proportional to the diameter  $D$  of the array, and the first “null” will be approximately at  $|\mathbf{K}| = K_{\min} = 2\pi/D$ . This main lobe width can be shown to define an on-axis angular resolution equal to  $\lambda/D$ , where  $\lambda$  is wavelength. At a measurement distance equal to  $L$  this angular resolution corresponds to a spatial resolution,  $R$  given by the expression

$$R = \frac{L}{D} \lambda \quad (4)$$

The measurement distance  $L$  should not be much smaller than the array diameter  $D$ . For comparison, NAH provides a resolution around  $\lambda/2$  at high frequencies and approximately equal to the measurement distance  $L$  at lower frequencies. Thus, at low frequencies NAH can provide significantly better resolution, when a sufficiently small measurement distance is used.

### 3. Beamforming with increased spatial resolution

Using iterative deconvolution techniques it is possible to achieve higher resolution than provided by standard DAS beamforming techniques<sup>(4)</sup>. The idea is that when measuring on a point source the DAS beamforming pressure power result is given by the location of the point source convolved by the Beamformers directional characteristics as shown in Fig. 1(b) and produces what is known as the point-spread function, PSF. For a given Beamformer array design, this PSF is known and can be compensated for using de-convolution techniques. This de-convolution gives a possibility to increase the spatial resolution of acoustic arrays and reduce disturbing side lobe effects. In many fields of imaging, like for example optical and radio astronomy, de-convolution methods are widely used to increase the spatial resolution. For that purpose a variety of algorithms has been developed in the past, for example Non Negative Least Squares, NNLS algorithm. It is within recent years that the algorithms have been applied to acoustic array measurements and some of the most promising ones are the fast spatial FFT based De-convolution Approach for Mapping Acoustic Sources version 2, DAMAS2 and the FFT-NNLS. From a practical point of view there are only minor differences between the two approaches, except that FFT-NNLS is a little slower but often more precise than DAMAS2.

The steps of the algorithms are visualized in the followed: For a given array design monopoles are placed at a grid of positions covering the mapping area on the source plane. For

each monopole position,  $i$ , a Delay-and-Sum (DAS) beamforming measurement is simulated and the pressure power distribution on the source plane is calculated. Thus the  $\mathbf{PSF}_i$ , which only depends on the test geometry, is obtained for each source location,  $i$ . See Figs. 2 and 3 for two examples.

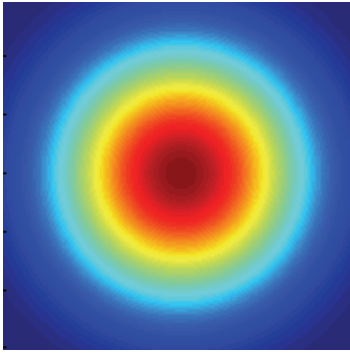


Fig. 2 – Point-Spread Function for an on-axis monopole at the focus plane

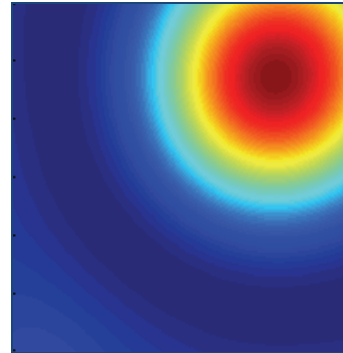


Fig. 3 – Point-Spread Function for a slightly off-axis monopole at the focus plane

For the actual array measurement an incoherent point source model is used and a solution is found in a least squares sense for non-negative monopole power strengths, i.e.  $A_i \geq 0$ , see Fig. 4.

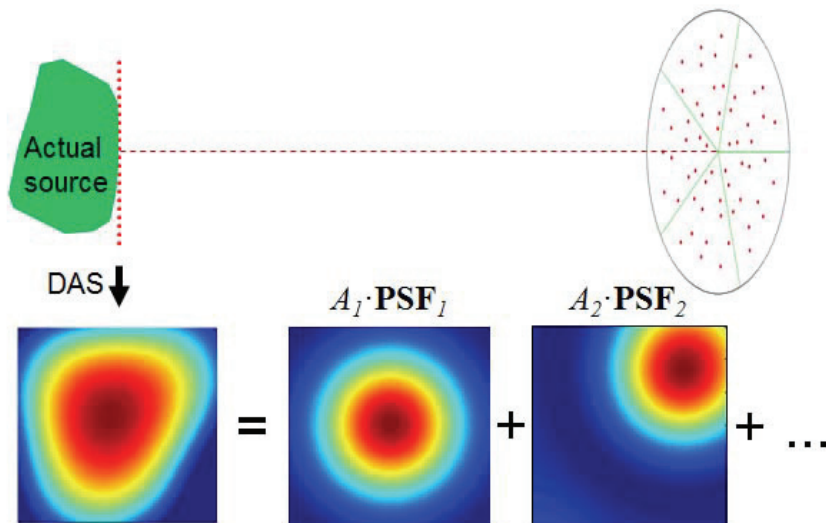


Fig. 4 – Incoherent source model is found in a least squares sense

The output from DAS is smeared by the individual  $\mathbf{PSF}_i$ . As an approximation, a position independent point-spread function (shift invariant across the mapping area) is assumed, so the one at the center of the mapping area  $\mathbf{PSF}_0$  is used in Eq. (5). Here,  $\mathbf{A} = \{A_i\}$  is a matrix containing all the source strengths, and the symbol  $\otimes$  represents convolution in  $x$  and  $y$ . Finally Eq. (5) is solved iteratively for  $\mathbf{A}$  (de-convolution), which means that in practice the spatial resolution is improved compared to the original DAS by a factor 3-10, depending on the geometry of the array and test object. In practice approximately 50 iteration steps are enough.

(5)

#### 4. Measurement examples of aerodynamic noise measurements

For beamforming measurements in wind tunnels, it is usual to place a half wheel on the floor of the tunnel in order to take advantage of the mirror ground condition. As the array is usually a few metres from the vehicle under test, it is also well outside the airflow region so wind induced noise is reduced. All the cross-spectra are measured simultaneously which enables the wind noise induced in the microphones to be eliminated by using only the cross terms in the complete cross spectrum matrix. The autospectra on the diagonal of this matrix are not used in the further calculation, this improves the S/N ratio. No references are necessary.

Fig. 5 shows a vehicle in a wind tunnel, where the sound distribution was investigated as a function of yaw angle. The vehicle was fully taped to reduce the effects of leakage around seals and to reduce turbulence produced by wheel arches, undercarriage etc. <sup>(5)</sup>.

Using a reference signal from, for example, a surface microphone positioned behind the side-mirror, effectively produces a selective beamformer; the noise from around the mirror and A-pillar will be accentuated, whereas the noise contribution from the turbulence produced by the front of the vehicle will be suppressed.



Fig. 5 – Wind tunnel with taped vehicle on rotating plate used to adjust yaw angle. Spherical Beamformer in the cabin, and Half Wheel Beamforming array at 3.8 m distance (0 degree yaw)

The main sources of aerodynamic noise perceived by the driver are usually the A-pillar and the side mirror. Therefore, exterior beamforming focuses on these areas. Figs. 6 and 7 show results using a full wheel, beamforming array hung above the roof of the vehicle and a half wheel array positioned facing the side of the vehicle respectively.

The results were calculated for two different beamforming algorithms. Delay-and-Sum, DAS is the most commonly used beamforming algorithm. Whereas the Non Negative Least Squares algorithm is a de-convolution method well known in other industries as mentioned earlier. As clearly seen in Fig. 6 NNLS offers better resolution at lower frequencies and better suppression of side lobes at higher frequencies compared to DAS.

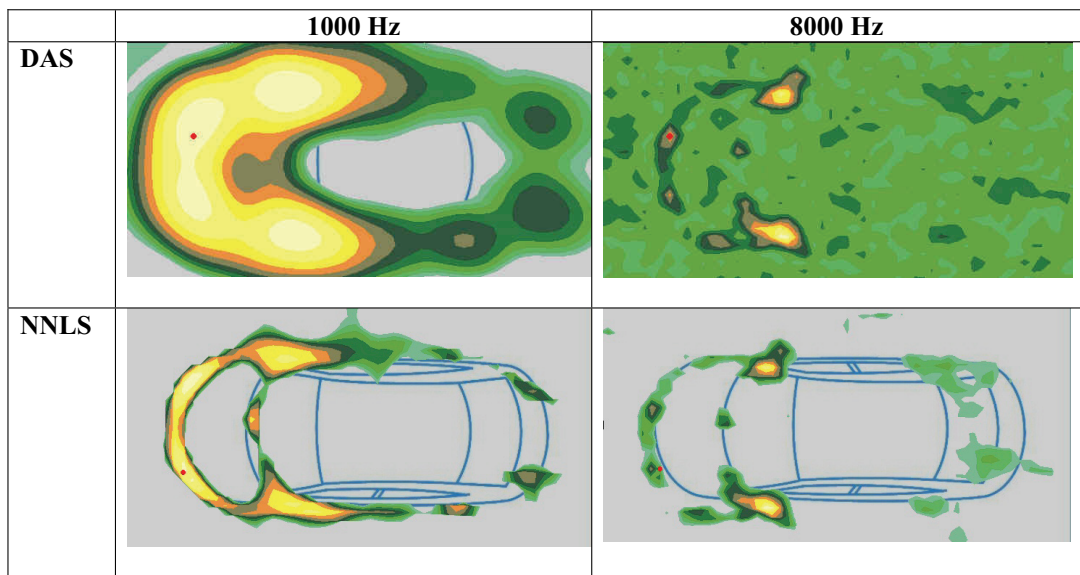


Fig. 6 – Wheel array supported above test vehicle in wind tunnel. 15 dB display range. NNLS yields better resolution at all frequencies and better suppression of side lobes at higher frequencies

In Fig. 7 sound maps around A-pillar and side mirror are shown for noise in 16 Hz bandwidths. Virtually no difference is noticed for the Delay and Sum results whereas the NNLS shows considerable frequency related detail.

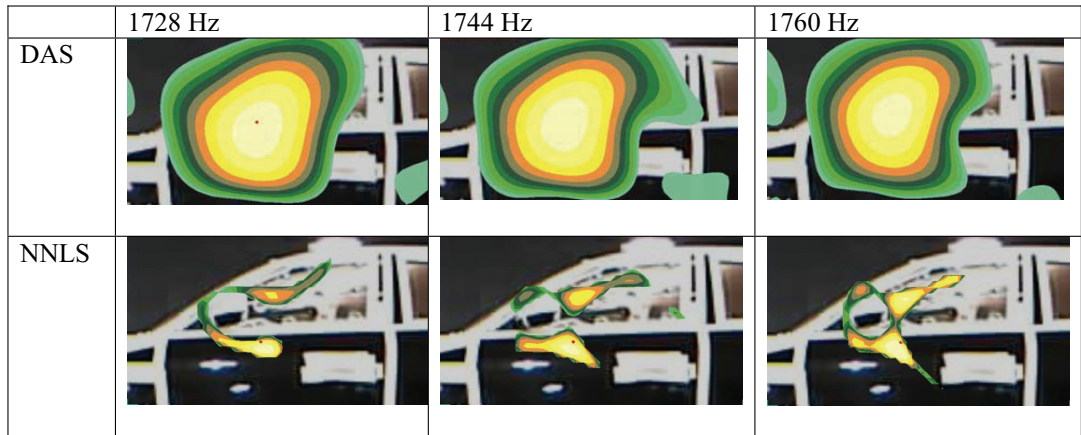


Fig. 7 – Low intrusion A-pillar and side mirror at -10 degrees yaw. 10 dB display range

## 5. Summary and Conclusions

In this paper it has been presented how additional de-convolution algorithms can be applied to traditional Delay-and-Sum, DAS measurements and calculations. This means users can add these algorithms to their existing measurements. The algorithms are efficient and fast FFT based NNLS (Non-negative Least Squares) and DAMAS2 (De-convolution Approach for Mapping Acoustic Sources ver. 2). As shown in the measurement examples from the automotive industry there are considerable improvements in both spatial resolution and in suppression of side lobe effects.

## REFERENCES

- <sup>1</sup> J. Hald and J.J. Christensen, “A novel beamformer design for noise source location from intermediate measurement distances”, *Proceedings of ASA/IFA/MIA* (2002)
- <sup>2</sup> J.J. Christensen and J. Hald, “Beamforming”, *Brüel & Kjær Technical Review no. 1*, pp. 1–48. (2004)  
<http://www.bksv.com/Library/Technical%20Reviews.aspx?year=2004-2000&st=2004-2000>
- <sup>3</sup> J. Hald, “Combined NAH and Beamforming using the same Array - SONAH”, *Brüel & Kjær Technical Review no. 1*, pp. 11–50. (2005)  
<http://www.bksv.com/Library/Technical%20Reviews.aspx?year=2012-2005&st=2012-2005>
- <sup>4</sup> Klaus Ehrenfried and Lars Koop, “A Comparison of Iterative Deconvolution algorithms for the Mapping of Acoustic Sources”, *American Institute of Aeronautics and Astronautics, AIAA Journal, Volume: 45, Issue: 7*, pp. 1584-1595 (2007)
- <sup>5</sup> Bernard Ginn and Jørgen Hald “Aerodynamic noise source identification in wind tunnels using acoustical array techniques” *8<sup>th</sup> MIRA International Vehicle Aerodynamics Conference - 'Low Carbon Vehicles'* (2010)